Main Menu

- Home
- Welcome
- Introductory Matters
- Program at a Glance
- Sessions
- Author Index
- Digest Book
- Instructions for use

WELCOME TO INTERMAG EUROPE 2008 CD

The INTERMAG Europe 2008 Conference is to be held in the *Palacio Municipal de Congresos de Madrid*, from **May 4 to May 8, 2008**.

Information related to the location, conference registration, publications, presentations, posters, etc can be found in the introductory sections of the Advance Program Book. For more information please check the conference web-site at http://www.intermagconference.com/intermag2008.

To view the digests of the papers to be presented at the conference you will need to have Adobe Acrobat Reader installed on your computer. If you do not have this available Click here to install the software on your laptop.

CL-10. A STUDY ON THE IRREVERSIBLE MAGNET DEMAGNETIZATION IN SINGLE-PHASE LINE-START PERMANENT MAGNET RELUCTANCE MOTOR. J. Hong[2], H. Nam[3] and *T. Kim[1] 1. Electrical Engineering, Gyeongsang National Unversity, Jinju, South Korea; 2. Hanyang Unversity, Seoul, South Korea; 3. LG Electronics, Changwon, South Korea*

CL-11. Design of IPM type BLDC motor considering demagnetization characteristics. *B. Yang[1]*, S. Hong[1] and B. Kwon[1] *1. Hanyang Unv., Ansan, South Korea*

CL-12. Characteristic analysis of Permanent Magnet Motor Considering Anisotropic Characteristics of Electrical Steel Sheets. *S. Kwon[1]*, J. Lee[1], K. Ha[2] and J. Hong[1] *1. Department of Mechanical Engineering, Hanyang Univeristy, Seoul, South Korea; 2. POSCO Technical Research Laboratories, Pohang, South Korea*

TUESDAY **POLIVALENTE**
MORNING
9:00

Session CM
MAGNETIC MICRO- AND NANOSTRUCTURES (POSTER SESSION)
Tom Thomson, Chair

A Study on the Irreversible Magnet Demagnetization in Single-Phase Line-Start Permanent Magnet Motor

Jung-Pyo Hong[1], *Senior Member, IEEE*, Hyuk Nam[2], *Member, IEEE*, and Tae Heoung Kim[3], *Member, IEEE*

[1]Department of Automotive Engineering, Hanyang University, Seoul 133-701, Korea
[2]LG Electronics, Changwon, Gyeongnam 641-711, Korea
[3]Department of Electrical Engineering, Engineering Research Institute, Gyeongsang National University, Jinju, Gyeongnam 660-701, Korea

The large demagnetizing currents in a single-phase line-start permanent magnet motor (LSPMM) are generated by a starting and locked rotor condition. So, irreversible magnet demagnetization occurs due to the external demagnetizing field by these currents.

In this paper, we present the phenomena of the irreversible magnet demagnetization using two-dimensional finite-element method (2-D FEM). The nonlinear analysis of a permanent magnet is added to 2-D FEM to consider irreversible demagnetization. As a result, design techniques which are effective to avoid irreversible demagnetization are proposed.

***Index Terms*—Brushless motor, FEM, permanent magnet, single-phase**

I. Introduction

SINGLE-PHASE LINE-START PERMANENT MAGNET MOTOR (LSPMM) are known to be capable of high efficiency and near unity power factor performance. These attributes make them an attractive choice for various high duty cycle applications [1], [2]. The LSPMM dose not need a driving system such as an inverter, because of the asynchronous starting torque by means of conductor bars in the rotor. However, the large currents at a starting or locked rotor condition can cause severe irreversible demagnetizing in the permanent magnet. This demagnetizing field deteriorates the performance of the LSPMM such as phase peak-to-peak variation [3]-[5]. Therefore, the demagnetization of the permanent magnet should be considered in the design of the rotor shape of the LSPMM. In this paper, we present the phenomena of the irreversible magnet demagnetization and propose design techniques which are effective to avoid irreversible demagnetization. To analyze the irreversible demagnetization of the magnet, two-dimensional finite-element method (2D FEM) is used. The nonlinear characteristic of the permanent magnet is considered as well as that of a magnetic core on each B-H curve.

II. Analysis Model

Fig. 1 shows the proto-type LSPMM with two-layer rear-earth permanent magnet. It has a 24-slot stator and a 2-pole rotor. In the rotor, there are permanent magnets and conductor bars to produce the starting torque. The permanent magnet material is sintered Nd-Fe-B. The air gap was designed to be 0.5 mm to obtain a reasonable permeance coefficient value. Table I summarizes the important LSPMM design specifications. The equivalent circuit of a LSPMM is shown in Fig. 2. The starting capacitance *Cs* , running capacitance *Cr* are connected to the auxiliary winding to increase the starting torque and power factor.

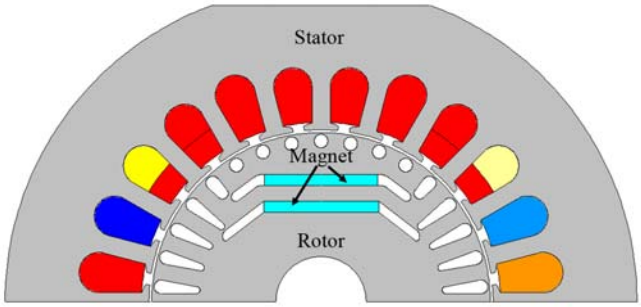

Fig. 1. The proto-type single-phase LSPMM.

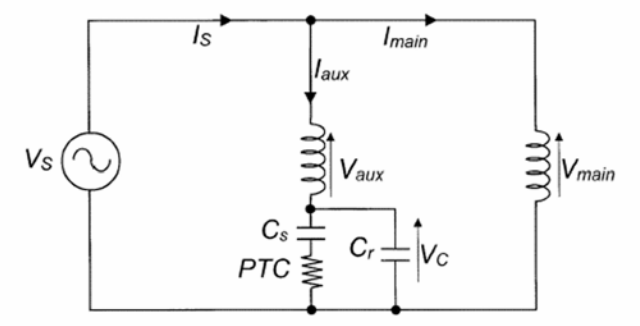

Fig. 2. Equivalent circuit of the single-phase LSPMM.

TABLE I
SPECIFICATIONS OF THE PROTOTYPE LSPMM

Section	Item	Value	(Unit)
Stator	Number of slots	24	
	Outer diameter	112	(mm)
	Stack width	90	(mm)
Rotor	Number of poles	2	
	Outer diameter	60	(mm)
Magnet	Material	Nd-Fe-B	
	Residual flux density (Br)	1.15	(T)
Air gap	Mechanical air gap	0.5	(mm)

Digital Object Identifier inserted by IEEE

III. Finite Element Method

A. Governing Equation and Discretization

The 2-dimensional governing equation for the LSPMM is expressed in a magnetic vector potential A as

$$\frac{\partial}{\partial x}\left(\frac{1}{\mu}\frac{\partial A_z}{\partial x}\right)+\frac{\partial}{\partial y}\left(\frac{1}{\mu}\frac{\partial A_z}{\partial y}\right)=-J_0-\left(\frac{\partial M_y}{\partial x}-\frac{\partial M_x}{\partial y}\right) \quad (1)$$

Where

A_z : Z component of magnetic vector potential

J_0 : Current density

M : Magnetization of the permanent magnet

Applying the Galerkin method to (1), we can obtain the finite element equation in a first order triangular element as follows:

$$I_{ie}=\int_{Se}\frac{1}{\mu}\sum_{j=1}^{3}\left(\frac{\partial N_{ie}}{\partial x}\frac{\partial N_{je}}{\partial x}+\frac{\partial N_{ie}}{\partial y}\frac{\partial N_{je}}{\partial y}\right)A_{je}\,dxdy$$
$$-\int_{Se}\frac{1}{\mu}\left(M_x^e\frac{\partial N_{ie}}{\partial y}-M_y^e\frac{\partial N_{ie}}{\partial x}\right)dxdy-\int_{Se}J_0N_{ie}\,dxdy \quad (2)$$

Where N stands for shape function.

B. Nonlinear Analysis of a Permanent Magnet

In order to perform the nonlinear calculation of a permanent magnet, we use the approximate equation for magnetization M of a magnet. Fig. 3(a) shows a typical demagnetization curve of permanent magnet materials. From this graph, we can find $H=f(B)$. Then, the approximate equation for magnetization M is derived as follows:

$$M=B-\mu_0H=B-\mu_0f(B)=h(B) \quad (3)$$

where M is magnetization of a permanent magnet and μ_0 is permeability. Equation (3) means that the magnetization M of a magnet is the function of flux density B. Fig. 3(b) shows the $M-B$ curve of permanent magnet.

Applying the Newton-Raphson method to (2), we can obtain the following equation to be related with equivalent magnetic current density J_{mi}.

$$\frac{\partial J_{mi}^e}{\partial A_{je}}=\frac{\nu_0}{4\Delta^e}\left(\frac{\partial M_x^e}{\partial B_x}d_{ie}d_{je}+\frac{\partial M_y^e}{\partial B_y}c_{ie}c_{je}\right) \quad (4)$$

where Δ^e is the area of an element and c and d are the coefficients that are related with the coordinate.

C. Phase Flux Linkage Calculation for Back-EMF

The phase flux linkage λ can be calculated from the average vector potential over each winding cross section [6].

$$\lambda=\left[\iint_{S_1}A_1dS/S_1-\iint_{S_2}A_2dS/S_2\right]l \quad (5)$$

Where l is the stack length and S_1 and S_2 represent the total areas of an N-turn winding carrying the positive current and negative current, respectively.

IV. Analysis and Test Results

A. Demagnetization curve

Fig. 3(a) also shows the procedure of demagnetization. When operating point P_1 moves to P_2 due to the external demagnetization field, the residual flux density B_r is decreased to B_r' , and irreversible magnet demagnetization occurs. As a result, the magnetization M of the magnet is also decreased.

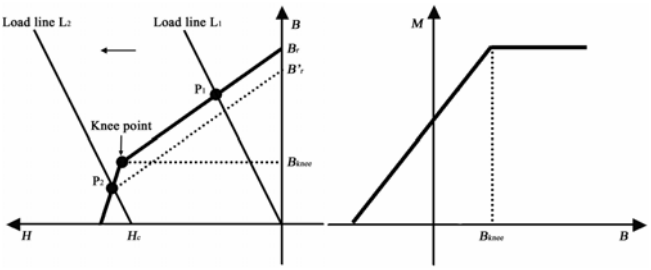

(a) Demagnetization curve (b) *M-B* curve

Fig. 3. Characteristic curve of permanent magnet.

B. Demagnetization phenomena

Fig. 4 and 5 show the demagnetization phenomena of the analysis model with the increase of stator magneto motive force (MMF). The magnet has initial 1.15T magnetization before demagnetization. However, it is decreased after demagnetization as shown in Fig. 3(a). From these figures, we can see that the magnet demagnetization becomes larger as the MMF increases. Firstly, the center part of the lower layer magnet is demagnetized as the MMF increases. And then, the overall regions of the lower layer magnet become demagnetized. Lastly, the regions of the upper layer magnet have an irreversible demagnetization. This is due to concentrated external demagnetization field on the lower layer magnet.

From these analysis results, we can know that more thick magnet in the lower layer compared to the upper layer is effective to avoid irreversible permanent magnet demagnetization. It is also possible to use different magnet materials in the upper and the lower layer. Fig. 6 illustrates the flux lines.

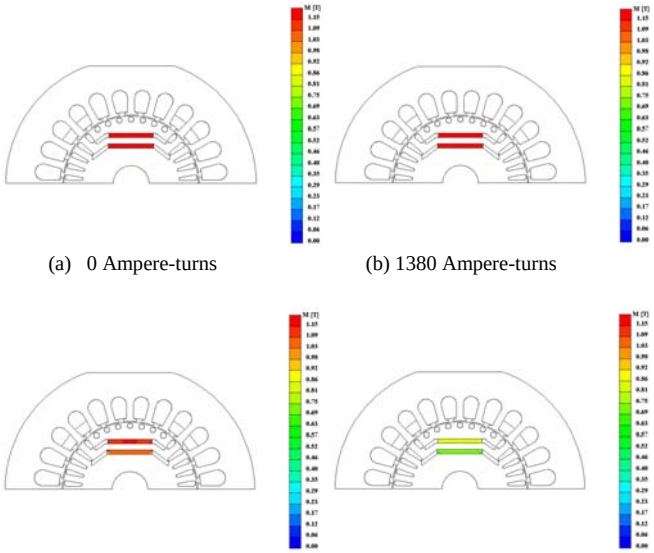

(a) 0 Ampere-turns (b) 1380 Ampere-turns

(c) 2760 Ampere-turns (d) 4140 Ampere-turns

Fig. 4. Magnetization distribution according to the MMF.

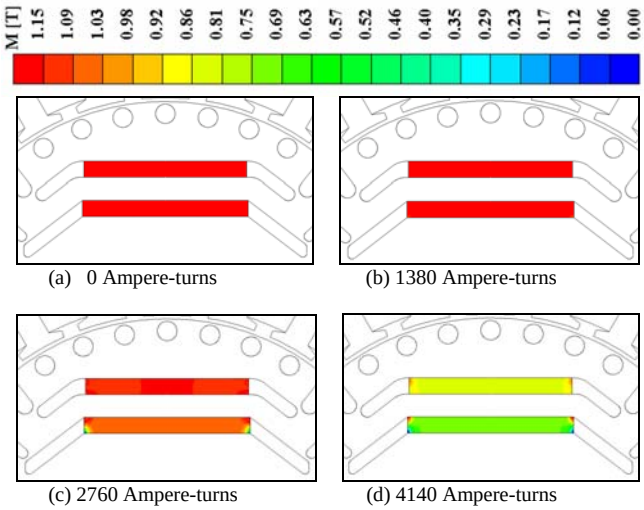

(a) 0 Ampere-turns (b) 1380 Ampere-turns

(c) 2760 Ampere-turns (d) 4140 Ampere-turns

Fig. 5. Zoomed magnetization distribution according to the MMF.

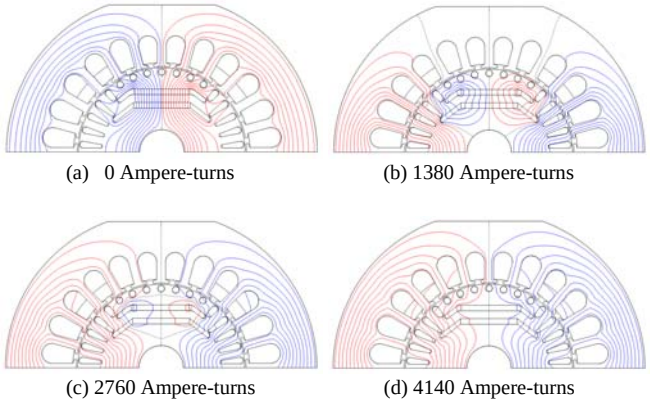

(a) 0 Ampere-turns (b) 1380 Ampere-turns

(c) 2760 Ampere-turns (d) 4140 Ampere-turns

Fig. 6. Flux lines.

C. Test results

To prove the propriety of the analysis method, we built the prototype LSPMM with Nd-Fe-B magnets and performed the experiment. The constructed rotor is shown in Fig. 7.

Fig. 8 compares the measured and the calculated back-EMF waveforms. The measurements were carried out at no-load by driving the LSPMM using a brushless permanent magnet servo motor. The experimental results closely match those obtained from the simulation of the analysis method. From these results, we know that the back-EMF is reduced because of demagnetization. After all, the irreversible magnet demagnetization deteriorates the LSPMM performance.

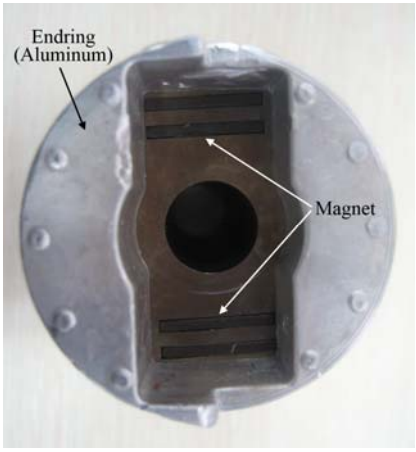

Fig. 7. The constructed rotor.

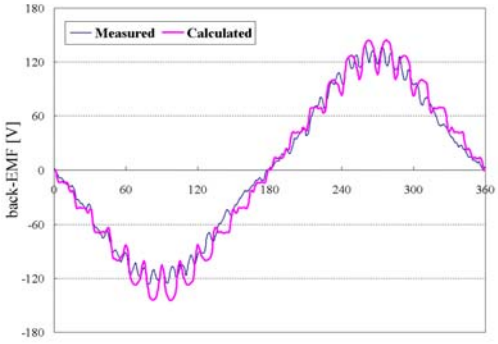

(a) Before demagnetization

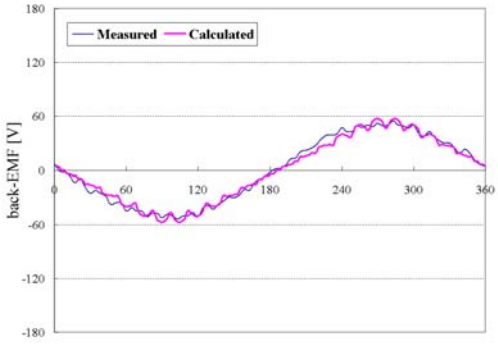

(b) After demagnetization

Fig. 8. Comparison of back-EMF.

V. Proposed Design Technique

Fig. 9 shows the 1/2 cross-sectional configuration of the proposed LSPMM. It has different thickness magnets in the upper and the lower layer to avoid irreversible demagnetization. The magnet thickness in each layer of the initial LSPMM is 2 (mm). However, the proposed LSPMM has 1.5 (mm) in the upper layer and 2.5 (mm) in the lower layer, respectively. The total magnet thicknesses are the same in each LSPMM.

Fig. 10 and 11 compare the magnetization distribution of the initial and that of the proposed LSPMM when MMF is 2760 and 4140 Ampere-turns, respectively. Fig. 12 and 13 show the calculated back-EMF. In the case of 2760 Ampere-turns, the proposed LSPMM is more effective to avoid the demagnetization. However, the effectiveness of the proposed design method decreases as the demagnetization current increases. This is because the effect of external demagnetization field on the upper layer magnet with the thin magnet becomes large. Accordingly, the selection of the proper magnet thickness considering the demagnetization current is needed and important.

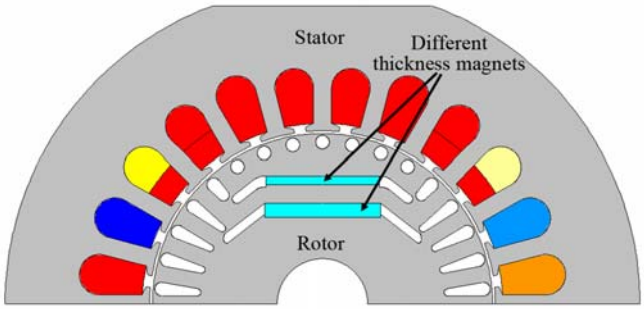

Fig. 9. Proposed LSPMM.

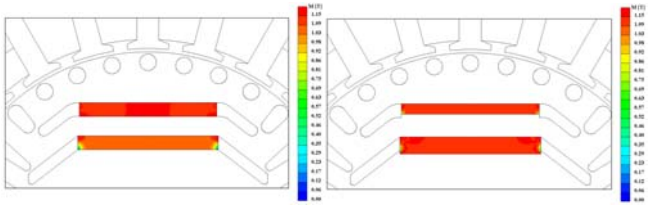

(a) Initial LSPMM (b) Proposed LSPMM

Fig. 10. Comparison of magnetization distribution. (2760 Ampere-turns).

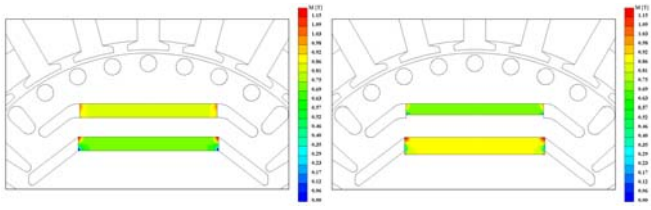

(a) Initial LSPMM (b) Proposed LSPMM

Fig. 11. Comparison of magnetization distribution. (4140 Ampere-turns).

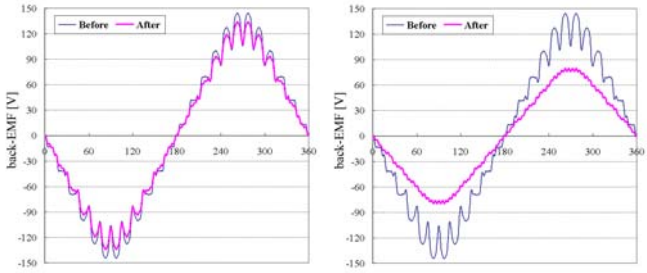

(a) 2760 Ampere-turns (b) 4140 Ampere-turns

Fig. 12. Comparison of back-EMF in the initial LSPMM.

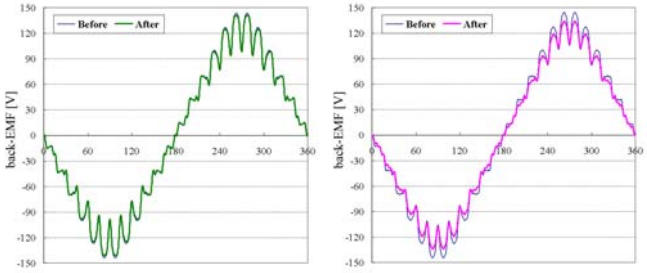

(a) 2760 Ampere-turns (b) 4140 Ampere-turns

Fig. 13. Comparison of back-EMF in the proposed LSPMM.

VI. Conclusion

An effective design technique to avoid irreversible permanent magnet demagnetization of a LSPMM has been proposed and studied both theoretically and experimentally. The nonlinear characteristic of a permanent magnet is considered as well as that of a magnetic core on each B-H curve. It is also shown that irreversible magnet demagnetization reduces back-EMF and deteriorates the performance of a LSPMM.

We confirm that our proposed method is useful for the design of a LSPMM with high performance.

References

[1] T. J. E. Miller, “Single-phase permanent magnet motor analysis,” *IEEE Trans. Ind. Applica.*, vol. IA-21, no. 4, pp. 651-658, 1985.

[2] M. A. Rahman and P. Zhou, “Analysis of brushless permanent magnet synchronous motors,” *IEEE Trans. Ind. Electron.*, vol. 43, no. 2, pp. 256-267, 1996.

[3] G. H. Kang *et al.*, “Improved parameters modeling of interior permanent magnet synchronous motor by finite element analysis,” *IEEE Trans. Magn.*, vol. 36, pp. 1867-1870, July 2000.

[4] H. C. Lovatt and P. A. Watterson, “Energy stored in permanent magnets,” *IEEE Trans. Magn.*, vol. 35, pp. 505-507, January 1999.

[5] G. H. Kang, J. Hur, H. Nam, J. P. Hong, and G. T. Kim, “Analysis of Irreversible Magnet Demagnetization in Line-Start Motors Based on the Finite-Element Method,” *IEEE Trans. Mag.*, vol. 39, no. 3, pp. 1488-1491, May 2003.

[6] L. Chang, “In improved FE inductance calculation for electrical machine,” *IEEE Trans. Magn.*, vol. 32, no. 4, pp. 3237-3245, 1996.

Manuscript received March 3, 2008. Corresponding author: Tae Heoung Kim (e-mail: ktheoung@gnu.ac.kr; phone: +82-55-751-5349).